

# Multi-level Matching Network for Multimodal Entity Linking

Zhiwei Hu

School of Computer and Information Technology  
Shanxi University  
Taiyuan, China  
zhiwei.hu@whu.edu.cn

Ru Li\*

School of Computer and Information Technology  
Shanxi University  
Taiyuan, China  
liru@sxu.edu.cn

Víctor Gutiérrez-Basulto\*

School of Computer Science and Informatics  
Cardiff University  
Cardiff, UK  
gutierrezbasultov@cardiff.ac.uk

Jeff Z. Pan\*

ILCC, School of Informatics  
University of Edinburgh  
Edinburgh, UK  
j.z.pan@ed.ac.uk

## ABSTRACT

Multimodal entity linking (MEL) aims to link ambiguous mentions within multimodal contexts to corresponding entities in a multimodal knowledge base. Most existing approaches to MEL are based on representation learning or vision-and-language pre-training mechanisms for exploring the complementary effect among multiple modalities. However, these methods suffer from two limitations. On the one hand, they overlook the possibility of considering negative samples from the same modality. On the other hand, they lack mechanisms to capture bidirectional cross-modal interaction. To address these issues, we propose a **Multi-level Matching network for Multimodal Entity Linking (M<sup>3</sup>EL)**. Specifically, M<sup>3</sup>EL is composed of three different modules: (i) a *Multimodal Feature Extraction* module, which extracts modality-specific representations with a multimodal encoder and introduces an intra-modal contrastive learning sub-module to obtain better discriminative embeddings based on uni-modal differences; (ii) an *Intra-modal Matching Network* module, which contains two levels of matching granularity: *Coarse-grained Global-to-Global* and *Fine-grained Global-to-Local*, to achieve local and global level intra-modal interaction; (iii) a *Cross-modal Matching Network* module, which applies bidirectional strategies, *Textual-to-Visual* and *Visual-to-Textual* matching, to implement bidirectional cross-modal interaction. Extensive experiments conducted on WikiMEL, RichpediaMEL, and WikiDiverse datasets demonstrate the outstanding performance of M<sup>3</sup>EL when compared to the state-of-the-art baselines.

## CCS CONCEPTS

• **Information systems** → **Multimedia databases**; **Multimedia information systems**; **Data mining**; • **Computing methodologies** → **Knowledge representation and reasoning**.

## KEYWORDS

Multimodal Entity Linking, Contrastive Learning, Multimodal Matching

## 1 INTRODUCTION

Entity Linking (EL) aims at aligning the mentions within a context to the corresponding entities in a knowledge base [15, 35].

\*Contact Authors.

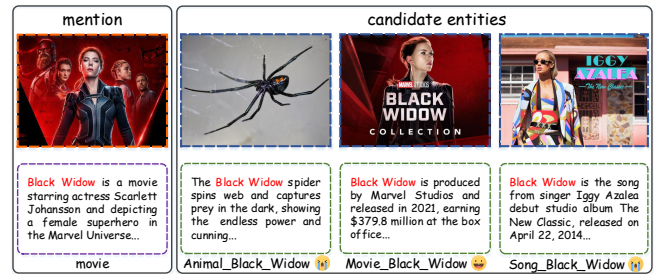


**Figure 1: An example of MEL. Dotted boxes of different colors represent different features: color purple for mention textual description (mention text), color orange for mention visual context (mention image), color green for entity textual description (entity text), color blue for entity visual context (entity image).**

EL supports numerous downstream information-retrieval applications, such as question answering [18, 26, 44, 45, 49], semantic search [4, 7, 13], dialog systems [2, 24], and so on [12, 17]. Most existing EL frameworks focus on mention disambiguation via context resolution in the textual modality. However, for multimodal information including images along with text, conventional text-based approaches to EL struggle to effectively encode such complex content. Multimodal Entity Linking (MEL) extends traditional EL by considering multimodal information, i.e., it aims at linking textual and visual mentions into their corresponding entities in a multimodal knowledge base. For example, in Figure 1, the mention *Black Widow* can be linked to the entities *Animal\_Black\_Widow*, *Movie\_Black\_Widow* and *Song\_Black\_Widow*. Although, it is possible to roughly guess the entity to which the mention has to be linked by relying solely on the textual description, the associated visual information can be used to improve the confidence of text-based predictions. Indeed, the image associated to the mention *Black Widow* has a high degree of semantic similarity with that of the entity *Movie\_Black\_Widow*, both including the actress *Scarlett Johansson*, which substantially increases the probability that the mention *Black Widow* is linked to the entity *Movie\_Black\_Widow*.

A wide variety of approaches to MEL have been already proposed, including representation learning (RL) frameworks [1, 29, 40, 43, 46, 50], vision-and-language pre-training (VLP) based methods [9,

19, 23, 28, 33], and a generative-based method [36]. Despite the substantial progress achieved so far, each of these approaches have their own disadvantages. The generative-based method GEMEL [36] leverages the in-context learning capability of large language models (LLMs) to create demonstrations, which requires a substantial amount of time and space overhead, and its performance is unsatisfactory. RL-based methods explore complementary effects of different modalities via joint or collaborative representation learning, e.g., using the concatenation operation [1], additive attention [29] or cross-attention mechanisms [40]. However, the above methods fail to integrate the information from pre-trained visual and textual models into the model representation process. VLP-based methods use a model jointly pre-trained on visual and language tasks as a modal encoder, although it can better understand the association between textual and visual information, they still suffer of two problems:

- (1) **Diversity of Negative Samples.** To learn better textual and visual embeddings, VLP models like CLIP [33] introduce a contrastive loss bringing paired image-text representations together, while pushing unpaired instances away from each other. However, they overlook the possibility of using negative samples from the same modality. Indeed, VLP-based MEL methods directly apply a VLP model as the textual and visual encoder, disregarding intra-modal negative samples. However, for the MEL task, both mentions and candidate entities contain independent textual and visual information. Implementing entity-mention interaction within the textual or visual modality is a natural way to improve the model representation capabilities.
- (2) **Bidirectional Cross-modal Interaction.** Existing methods only consider a one-way information flow, from textual to visual or visual to textual, during cross-modal interaction, i.e., they lack bidirectional cross-modal interaction. In practice, the textual-to-visual flow focuses more on the impact of the textual knowledge on the visual modality, while visual-to-textual pays attention to applying visual knowledge to the text modality. Therefore, we advocate that it is necessary to design a mechanism that better captures the bidirectional interaction pattern, to fully harness the knowledge of all available modalities.

To address the above two shortcomings, we propose a **Multi-level Matching network for Multimodal Entity Linking (M<sup>3</sup>EL)**. M<sup>3</sup>EL includes the following three modules. The *Multimodal Feature Extraction* module utilizes a pre-trained CLIP model to obtain modality-specific representations for each entity and mention. To alleviate shortcoming (1), we introduce an *Intra-modal Contrastive Learning* module to include negative samples within a modality into the discriminative embedding acquisition process. Additionally, we employ an *Intra-modal Matching Network* module which contains two levels of matching granularity, *Coarse-grained Global-to-Global* and *Fine-grained Global-to-Local* matching, to realize the interaction between local and global features within a modality. Moreover, we design a *Cross-modal Matching Network* module which considers bidirectional matching strategies, *Textual-to-Visual* and *Visual-to-Textual* matching, to reduce the gap between the distribution over different modalities, addressing shortcoming (2).

- We propose the M<sup>3</sup>EL framework for MEL, which simultaneously considers the diversity of negative samples and bidirectional cross-modal interaction.
- We introduce an intra-modal contrastive learning mechanism to obtain better discriminative embedding representations that are faithful within a modality.
- We devise intra-modal and cross-modal matching networks to explore different multimodal interactions, reducing the gap over intra-modality and cross-modality distributions.
- We conduct a series of empirical and ablation experiments on three well-known datasets, showing the strong performance of M<sup>3</sup>EL when compared to the state-of-the-art. Code and data are available at: <https://github.com/zhiwei1103/MEL-M3EL>.

## 2 RELATED WORK

► **Entity Linking.** Recent methods for Entity Linking (EL) mainly focus on exploiting ambiguous mentions to the referent unambiguous entities in a given knowledge base, which can be divided into two series: *local-level* methods and *global-level* methods. Local-level methods [5, 32, 42] primarily consider mention along with its surrounding words or sentence to capture contextual information. Global-level methods [6, 10, 11, 20, 34, 48] also take entity or topic coherence into account to calculate the mention and entity semantic consistency. However, these methods do not work well when processing multimodal data, including textual and visual content.

► **Multimodal Entity Linking.** Multimodal entity linking is an extension of the traditional entity linking task that utilizes additional multimodal information (e.g., visual information) to support the disambiguation of entities. Mainstream approaches can be classified into two categories: Representation Learning (RL) frameworks and Vision-and-Language Pre-training (VLP) methods. (i): *RL-based methods*: DZMNEED [29] utilizes a multimodal attention mechanism to fuse textual, visual and character features of mentions and entities. JMEL [1] introduces fully connected layers to embed the textual and visual information into an implicit joint space. VELML [50] designs a deep modal-attention neural network to aggregate different modality features and map visual objects to the entities. GHMFC [40] extracts the hierarchical features of textual and visual co-attention through a multi-modal co-attention mechanism. DRIN [43] explicitly encodes four different types of alignments between mentions and entities, and builds graph convolutional network to dynamically select the corresponding alignment relations for different input samples. MMEL [46] proposes a joint feature extraction module to learn textual and visual representations, and a pairwise training schema and multi-mention collaborative ranking mechanism to model the potential connections. (ii): *VLP-based models*: CLIP [33] trains on large-scale image-caption pairs with contrastive self-supervised objectives to attain textual and visual representations. ViLT [19] discards convolutional visual features and adopts a vision transformer to model long-range dependencies over a sequence of fixed-size non-overlapping image patches. ALBEF [23] introduces a contrastive loss to align the textual and visual representations before fusing them through cross-modal attention to enable more grounded vision and language representation learning. METER [9] systematically investigates how to train

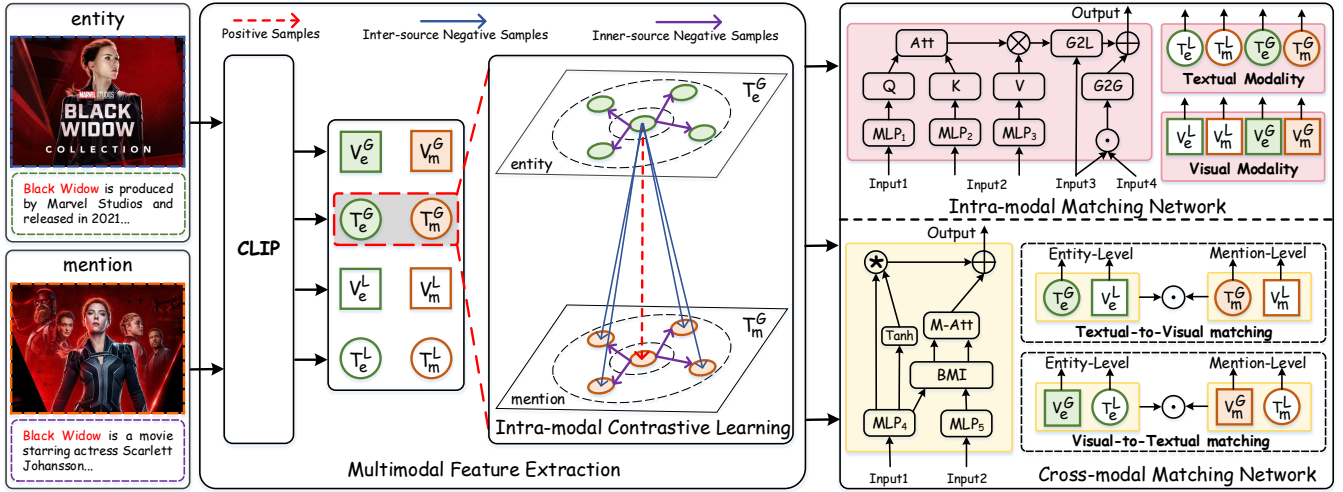


Figure 2: The structure of the  $M^3EL$  model, containing three modules: Multimodal Feature Extraction (MFE) with Intra-modal Contrastive Learning (ICL), Intra-modal Matching Network (IMN) and Cross-modal Matching Network (CMN). *Att* and *M-Att* denote the attention and multi-heads attention mechanisms, respectively.

a full-transformer vision-language pre-trained model in an end-to-end manner. MIMIC [28] utilizes BERT [8] and CLIP as textual and visual encoder, respectively, and organizes three interaction mechanisms to comprehensively explore the intra-modal and inter-modal interaction among embeddings of entities and mentions. (iii): *generative-based method*: GEMEL [36] leverages the in-context learning capability of LLMs (e.g., LLaMa-2-7B [37]) by retrieving multimodal instances as demonstrations, and then applies a constrained decoding strategy to efficiently search the valid entity space. Considering that it requires the use of an LLM with intensive computation and parameters, this poses a great challenge to the efficiency of GEMEL. Furthermore, there is a large gap between its performance and the state-of-the-art. Therefore, generative-based method is not mainstream and is still in an exploration phase. Although existing RL-based or VLP-based methods have made significant progress, they still have two limitations that need to be addressed: On the one hand, VLP-based MEL methods directly utilize VLP as the textual and visual encoder, however VLP does not consider negative samples within a modality during the pre-training process. Both entities and mentions in the MEL task contain textual and visual knowledge. Considering negative samples of entities and mentions in the same modality is useful for improving contrastive learning capabilities. On the other hand, existing methods only consider the information flow from textual to visual or from visual to textual when interacting between modalities, and lack bidirectional cross-modal interaction.

### 3 METHOD

In this section, we first define the task of multimodal entity linking, and then introduce the  $M^3EL$  framework, including: Multimodal Feature Extraction, Intra-modal Matching Network, and Cross-modal Matching Network.

#### 3.1 Task Definition

► **Multimodal Entity Linking.** Let  $\mathcal{E}$  be a set of entities in a multimodal knowledge base  $\mathcal{K}$ . Each entity  $E_e \in \mathcal{E}$  is of the form  $\{N_e, T_e, V_e\}$ , where  $N_e$  denotes the name of the entity,  $T_e$  is a textual description of the entity and  $V_e$  represents the visual context of the entity associated with its textual description. A *mention*  $E_m$  (and its context) is of the form  $\{N_m, T_m, V_m\}$ , where  $N_m$ ,  $T_m$ , and  $V_m$  respectively are the name of the mention, the token sequence in which the mention is located, and the corresponding visual image of the mention. The *multimodal entity linking (MEL) task* aims to retrieve the ground truth entity  $E_e \in \mathcal{E}$  that is the most relevant to the mention  $E_m$ . For example, in Figure 1, the mention *Black Widow* requires to be linked to one of the three candidate entities in the set  $\{Animal\_Black\_Widow, Movie\_Black\_Widow, Song\_Black\_Widow\}$ . After combining the textual description and visual information, we can conclude that the entity *Movie\\_Black\\_Widow* is the most relevant for the mention. Usually, the MEL task can be formulated by maximizing the log-likelihood over the training set  $\mathcal{D}$  as:

$$\varrho^* = \max_{\varrho} \sum_{(E_m, E_e) \in \mathcal{D}} \log \text{sim}(E_e | E_m, \mathcal{E}) \quad (1)$$

where  $\text{sim}(\cdot)$  calculates the similarity between the mention  $E_m$  and entity  $E_e$ , and  $\varrho$  represents the parameters involved in the optimization process,  $\varrho^*$  denotes the final model.

#### 3.2 MFE: Multimodal Feature Extraction

3.2.1 *Multi-modal Embeddings.* For an entity  $E_e$ , we treat its textual description  $T_e$  and visual context  $V_e$  as a text-image pair  $P_e = \{T_e; V_e\}$ . We similarly obtain the text-image pair representation of a mention:  $P_m = \{T_m; V_m\}$ . As feature extractor in  $P_e$  and  $P_m$ , we utilize a pre-trained CLIP model [33], which trains two neural-network-based encoders using a contrastive loss to match pairs of texts and images. More precisely, take  $P_e$  as an example, we obtain textual and visual embedding representations as follows:

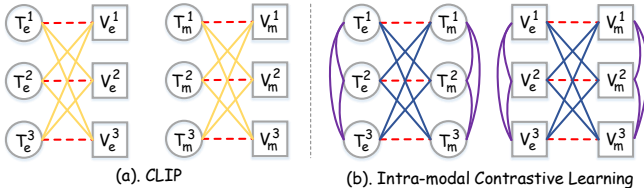


**Figure 3: Illustrative comparison of intra-modal contrastive learning with CLIP, where the red dashed lines represent the positive samples, yellow lines denote the negative samples in CLIP, purple and blue lines represent the inner-source and inter-source negative samples. Circles and squares represent textual and visual features,  $e$  and  $m$  represent entity and mention, respectively.**

► **Textual Modal Embedding.** We first concatenate the entity name  $N_e$  and the corresponding textual description  $T_e$  using the special tokens [EOT] and [SEP] to obtain the input sequence  $\{[EOT]N_e[SEP]T_e[SEP]\}$ . Then, we tokenize the input sequence to the token sequence  $\{t_e^{[EOT]}, t_e^1, t_e^2, \dots, t_e^l\}$ , where  $l+1$  is the length of the token sequence. Additionally, we use CLIP’s text encoder to extract the hidden states:  $\{t_e^{[EOT]}, t_e^1, t_e^2, \dots, t_e^l\} \in \mathbb{R}^{(l+1) \times d_t}$ , where  $d_t$  is the dimension of textual features. Finally, we consider the embedding of [EOT] as the global textual feature  $\mathbf{T}_e^G \in \mathbb{R}^{d_t}$  and the entire hidden state embeddings as local textual features  $\mathbf{T}_e^L \in \mathbb{R}^{(l+1) \times d_t}$ .

Similarly, we can also obtain the global textual feature  $\mathbf{T}_m^G$  and local textual feature  $\mathbf{T}_m^L$  of the mention textual modality.

► **Visual Modal Embedding.** Given an entity image  $V_e \in \mathbb{R}^{C \times H \times W}$ , we reshape  $V_e$  into a sequence of image patches  $\mathcal{V} = \{v_e^1, v_e^2, \dots, v_e^n\} \in \mathbb{R}^{n \times (P^2 \cdot C)}$ , where  $H \times W$  is the original image resolution,  $C$  is the number of channels,  $P \times P$  represents the patch image resolution,  $n = HW/P^2$  is the number of patches. We also prepend an additional [CLS] token to  $\tau$  before the image patches to represent the visual global feature, the corresponding patches sequence becomes  $\mathcal{V}' = \{v_e^{[CLS]}, v_e^1, v_e^2, \dots, v_e^n\}$ . We feed  $\mathcal{V}'$  into the CLIP visual encoder and further apply a fully connected layer to convert the dimension of the output hidden status into  $d_v$ . The corresponding embedding is denoted as  $\{v_e^{[CLS]}, v_e^1, v_e^2, \dots, v_e^n\} \in \mathbb{R}^{(n+1) \times d_v}$ . We take the embedding of the special token [CLS] as the global feature  $\mathbf{V}_e^G \in \mathbb{R}^{d_v}$  and the full embedding as local features  $\mathbf{V}_e^L \in \mathbb{R}^{(n+1) \times d_v}$ , where  $d_v$  is the dimension of the visual features.

Similarly, we can also obtain the global visual feature  $\mathbf{V}_m^G$  and local visual feature  $\mathbf{V}_m^L$  of the mention visual modality.

**3.2.2 Intra-modal Contrastive Learning.** CLIP learns a joint vision-language embedding space by bringing matching image-text representations together, while pushing unpaired instances away from each other. However, CLIP lacks an explicit mechanism that ensures that similar features from the same modality stay close in the joint embedding [3, 47, 52]. For example in Figure 3, given the entity textual feature  $\mathbf{T}_e^i$ , entity visual feature  $\mathbf{V}_e^i$ , mention textual feature  $\mathbf{T}_m^i$  and mention visual feature  $\mathbf{V}_m^i$ , CLIP only considers negative samples of  $\mathbf{T}_e^i$  from different modalities (i.e.,  $\mathbf{V}_e^j$  for  $j \neq i$ ), ignoring the possibility of having negative samples from the same modality, i.e.,  $\mathbf{T}_e^j$  and  $\mathbf{T}_m^j$ . CLIP is able to map image-text pairs

close together in the embedding space, while it fails to ensure that similar inputs from the same modality stay close by, which may result in degraded representations [47, 52]. However, the main aim of multimodal entity linking is to retrieve the ground truth entity most relevant to the mention, so simply considering the interaction between different modalities will inevitably lead to a one-sided embedding representation. Thus, it is necessary to consider the semantic difference between positive and negative samples within the same modality. To obtain better discriminative embedding representations that are faithful to unimodal differences, we introduce an Intra-modal Contrastive Learning module (ICL), composed of the following two steps:

► **Step 1. Obtaining Positive and Negative Samples.** We take the textual modality as an example. Assume that there are  $u$  entity textual descriptions  $\{T_e^1, T_e^2, \dots, T_e^u\}$  and  $u$  mention textual descriptions  $\{T_m^1, T_m^2, \dots, T_m^u\}$ , we can obtain the global textual feature corresponding to each piece of text based on the *Textual Modal Embedding* in Section 3.2.1. Note that for computational efficiency, we only perform intra-modal contrastive learning on the global feature level, we leave the interaction of local features to the *Intra-modal Matching Network* in Section 3.3. Furthermore, we found out that introducing contrastive learning at the local feature level will actually lead to performance degradation. Therefore, we omit superscripts  $G$  and  $L$  from textual embeddings of entities and mentions and simply denote them as  $\{\mathbf{T}_e^1, \mathbf{T}_e^2, \dots, \mathbf{T}_e^u\}$  and  $\{\mathbf{T}_m^1, \mathbf{T}_m^2, \dots, \mathbf{T}_m^u\}$ . For the entity embedding  $\mathbf{T}_e^i$ , the matching mention embedding  $\mathbf{T}_m^i$  provides a positive sample, while the embeddings of other entities and mentions are regarded as negative samples. More precisely, negative samples come from two sources: inner-source from the entity aspect and inter-source from the mention aspect. Inner-source means that the negative samples for  $\mathbf{T}_e^i$  are entity embeddings  $\mathcal{N}_e = \{\mathbf{T}_e^j \mid i \neq j\}$  in the same entity view where  $\mathbf{T}_e^i$  is located, while inter-source means that the negative samples are the embeddings  $\mathcal{N}_m = \{\mathbf{T}_m^j \mid i \neq j\}$  in the mention view where  $\mathbf{T}_e^i$  is not located.

► **Step 2. Contrastive Learning Loss Computation.** Take the entity textual embedding  $\mathbf{T}_e^i$  and the mention textual embedding  $\mathbf{T}_m^i$  as an example, we define the intra-modal contrastive learning loss of the positive pair  $(\mathbf{T}_e^i, \mathbf{T}_m^i)$  as follows:

$$\begin{cases} \mathcal{L}(\mathbf{T}_e^i, \mathbf{T}_m^i) = -\log \frac{\theta(\mathbf{T}_e^i, \mathbf{T}_m^i)}{\theta(\mathbf{T}_e^i, \mathbf{T}_m^i) + \beta \cdot \Phi_{inner} + \gamma \cdot \Phi_{inter}} \\ \Phi_{inner} = \sum_{\mathbf{T}_e^j \in \mathcal{N}_e} \theta(\mathbf{T}_e^i, \mathbf{T}_e^j) \\ \Phi_{inter} = \sum_{\mathbf{T}_m^j \in \mathcal{N}_m} \theta(\mathbf{T}_e^i, \mathbf{T}_m^j) \end{cases} \quad (2)$$

where  $\theta(x, y) = e^{\delta(x, y)/\tau}$ ,  $\tau$  is a temperature parameter,  $\delta(x, y)$  is the cosine similarity to measure the distance between two embeddings [16, 51, 52]. The  $\Phi_{inner}$  and  $\Phi_{inter}$  in the denominator sum up the inner-source and inter-source intra-modal negative samples, respectively.  $\beta$  and  $\gamma$  are the hyper-parameters to control the inner-source and inter-source alignment importance, respectively. While the nominator is symmetric, the denominator is not, so for the positive pair  $(\mathbf{T}_m^i, \mathbf{T}_e^i)$ , the corresponding intra-modal loss is  $\mathcal{L}(\mathbf{T}_m^i, \mathbf{T}_e^i)$ .

Similarly, for the visual positive sample pairs  $(\mathbf{V}_e^i, \mathbf{V}_m^i)$  and  $(\mathbf{V}_m^i, \mathbf{V}_e^i)$ , the corresponding contrastive losses are  $\mathcal{L}(\mathbf{V}_e^i, \mathbf{V}_m^i)$  and

$\mathcal{L}(\mathbf{V}_m^i, \mathbf{V}_e^i)$ . The final loss is the average of all textual and visual modalities pair losses, denoted as:

$$\mathcal{L}_{cl} = \text{avg}(\sum_i [\mathcal{L}(\mathbf{T}_e^i, \mathbf{T}_m^i) + \mathcal{L}(\mathbf{T}_m^i, \mathbf{T}_e^i) + \mathcal{L}(\mathbf{V}_e^i, \mathbf{V}_m^i) + \mathcal{L}(\mathbf{V}_m^i, \mathbf{V}_e^i)]) \quad (3)$$

### 3.3 IMN: Intra-modal Matching Network

Through the CLIP encoder, we can obtain global and local features of textual and visual modalities. Most previous works either exploit global features while overlooking the local features, or measure the local feature similarity whereas ignoring the global coherence [42]. MIMIC [28] considers the interaction between global and local features but it uses different independent mechanisms for the textual and visual modalities, making the global and local interaction deeply coupled with the modality. To alleviate the deep coupling between the interaction strategy and the modality type, we introduce the **Intra-modal Matching Network (IMN)** module to uniformly capture the interaction between local and global features within a modality. IMN contains two sub-modules, Coarse-grained **Global-to-Global** matching (**G2G**) and Fine-grained **Global-to-Local** matching (**G2L**). Take the textual modality as an example, using the CLIP encoder, we can obtain the entity global textual feature  $\mathbf{T}_e^G$ , entity local textual feature  $\mathbf{T}_e^L$ , mention global textual feature  $\mathbf{T}_m^G$  and mention local textual feature  $\mathbf{T}_m^L$ . We will use these features as the input to the G2G and G2L sub-modules.

► **Coarse-grained Global-to-Global matching.** To measure global consistency, we directly perform the dot product  $\odot$  between the entity global feature  $\mathbf{T}_e^G$  and the mention global feature  $\mathbf{T}_m^G$  to obtain the coarse-grained global-to-global matching score, formulated as:

$$\mathcal{M}_T^{G2G} = \mathbf{T}_e^G \odot \mathbf{T}_m^G \quad (4)$$

► **Fine-grained Global-to-Local matching.** We introduce an attention mechanism to explore the fine-grained clues among local features to obtain the fine-grained global-to-local matching score, formulated as:

$$\begin{cases} Q, K, V = \text{MLP}_1(\mathbf{T}_e^L), \text{MLP}_2(\mathbf{T}_m^L), \text{MLP}_3(\mathbf{T}_m^L) \\ \alpha^L = \text{Mean}(\text{Softmax}(\frac{Q \otimes K^T}{\sqrt{d_s}}) \otimes V) \\ \mathcal{M}_T^{G2L} = \mathbf{T}_e^G \odot \alpha^L \end{cases} \quad (5)$$

where  $\{\text{MLP}_1, \text{MLP}_2, \text{MLP}_3\}: \mathbb{R}^{d_t} \rightarrow \mathbb{R}^{d_s}$  are three multi-layer perceptron networks,  $d_s$  denotes the scaled dimension size,  $\otimes$  is the matrix multiplication operation,  $\text{Mean}(\cdot)$  represents the mean pooling operation,  $\alpha^L$  is the attention score generated from local features to impose constraints on global features.

Afterwards, we average the global-to-global and global-to-local matching scores to obtain the textual intra-modal matching score  $\mathcal{M}_T = (\mathcal{M}_T^{G2G} + \mathcal{M}_T^{G2L})/2$ . Similarly, for the visual modality, we can obtain the global-to-global matching score  $\mathcal{M}_V^{G2G}$  and global-to-local matching score  $\mathcal{M}_V^{G2L}$ , and the final combined matching score  $\mathcal{M}_V = (\mathcal{M}_V^{G2G} + \mathcal{M}_V^{G2L})/2$ .

### 3.4 CMN: Cross-modal Matching Network

Since the embeddings of different modalities are separately matched in the IMN module, it is difficult to model the complex interaction

between modalities solely based on an intra-modal matching mechanism. Although the CLIP model considers the alignment of information between multi-modalities, it is not specifically tailored for the MEL task. Therefore, it is necessary to appropriately adapt the inter-modal interaction to the embedding representation obtained from CLIP, based on the characteristics of the MEL task. To reduce the gap between the distribution over different modalities, we introduce the **Cross-modal Matching Network (CMN)** module, which contains two-way matching strategies: **Textual-to-Visual** matching (T2V) and **Visual-to-Textual** matching (V2T). Considering that the difference between T2V and V2T is only in the input embeddings content, we mainly give details for T2V. The T2V strategy has as input an entity-level textual-to-visual matching between the entity global textual feature  $\mathbf{T}_e^G$  and entity local visual features  $\mathbf{V}_e^L$ , and a mention-level textual-to-visual matching between the mention global textual feature  $\mathbf{T}_m^G$  and the mention local visual features  $\mathbf{V}_m^L$ . The entity-level and mention-level textual-to-visual matching mechanisms both include the following three steps. We use the entity-level to explain the details.

- (1) *Bidirectional Matching Interaction.* First, we employ a one-layer MLP to scale the dimensions of  $\mathbf{T}_e^G$  and  $\mathbf{V}_e^L$  to the same size. Then, we introduce an attention mechanism to obtain the local visual-aware global attention  $\mathbf{H}_e^{GL}$  and global textual-aware local attention  $\mathbf{H}_e^{LG}$ . Finally, we utilize the attention content to get an enhanced entity global textual feature  $\mathbf{T}_e^{G'}$   $\in \mathbb{R}^{d_c}$  and local visual features  $\mathbf{V}_e^{L'}$   $\in \mathbb{R}^{(n+1) \times d_c}$ . The entire interaction process is bidirectional since the data flows from local to global and global to local.

$$\begin{cases} \mathbf{T}_e^{\bar{G}} = \text{MLP}_4(\mathbf{T}_e^G), \mathbf{V}_e^{\bar{L}} = \text{MLP}_5(\mathbf{V}_e^L) \\ \mathbf{H}_e^{GL} = \text{Softmax}(\mathbf{T}_e^{\bar{G}} \otimes \mathbf{V}_e^{\bar{L}}), \mathbf{H}_e^{LG} = \text{Softmax}(\mathbf{V}_e^{\bar{L}} \otimes \mathbf{T}_e^{\bar{G}}) \\ \mathbf{T}_e^{G'} = \text{Relu}(\mathbf{H}_e^{GL} \otimes \mathbf{V}_e^{\bar{L}}), \mathbf{V}_e^{L'} = \text{Relu}(\mathbf{H}_e^{LG} \otimes \mathbf{T}_e^{\bar{G}}) \end{cases} \quad (6)$$

where  $\text{MLP}_4: \mathbb{R}^{d_t} \rightarrow \mathbb{R}^{d_c}$  and  $\text{MLP}_5: \mathbb{R}^{d_v} \rightarrow \mathbb{R}^{d_c}$  are multi-layer perceptron networks,  $d_c$  represents the scaled embedding dimension,  $\text{Softmax}(\circ)$  and  $\text{Relu}(\circ)$  are two different activation functions. To better understand Equation 6, we elaborate on the dimensional transformation occurring in it. It should be noted that to simplify the presentation, all dimensions do not include the batch size dimension, because the batch size of all operations is the same. (i): for the first row, we change  $\mathbf{T}_e^G \in \mathbb{R}^{d_t}$  and  $\mathbf{V}_e^L \in \mathbb{R}^{(n+1) \times d_v}$  to  $\mathbf{T}_e^{\bar{G}} \in \mathbb{R}^{d_c}$  and  $\mathbf{V}_e^{\bar{L}} \in \mathbb{R}^{(n+1) \times d_c}$ ; (ii): for the second row, we first extend the first dimension of  $\mathbf{T}_e^{\bar{G}}$  from  $\mathbb{R}^{d_c}$  to  $\mathbb{R}^{1 \times d_c}$ , then we perform a matrix multiplication operation on the expanded  $\mathbf{T}_e^{\bar{G}}$  and the transpose of  $\mathbf{V}_e^{\bar{L}}$ , and following the Softmax activation function to obtain  $\mathbf{H}_e^{GL} \in \mathbb{R}^{1 \times (n+1)}$ . Similarly, for  $\mathbf{H}_e^{LG} \in \mathbb{R}^{(n+1) \times 1}$ ; (iii): for the third row, we perform a matrix multiplication operation on  $\mathbf{H}_e^{GL} \in \mathbb{R}^{1 \times (n+1)}$  and  $\mathbf{V}_e^{\bar{L}} \in \mathbb{R}^{(n+1) \times d_c}$  to get  $\mathbf{T}_e^{G'} \in \mathbb{R}^{1 \times d_c}$  (for simplicity, we can omit the 1 in the dimension). Similarly, for  $\mathbf{V}_e^{L'} \in \mathbb{R}^{(n+1) \times d_c}$ .

- (2) *Multi-head Attention Fusion.* Given the enhanced entity local visual feature representation  $\mathbf{V}_e^{L'}$  and the enhanced entity global textual embedding  $\mathbf{T}_e^{G'}$ , we first concatenate them and then

introduce a multi-head attention mechanism to convert the concatenated vector  $\mathbf{h}_e^{T2V}$  into  $\mathbf{H}_e^{T2V} \in \mathbb{R}^{d_c}$ . Additionally, we apply a gate operation to fuse  $\mathbf{H}_e^{T2V}$  and the original entity global textual feature  $\mathbf{T}_e^G$  to obtain the entity-level textual-to-visual matching representation  $\mathcal{M}_e^{T2V}$ . More precisely, this process is formulated as follows:

$$\begin{cases} \mathbf{h}_e^{T2V} = \text{Concat}[\overline{\mathbf{V}}_e^{L'}; \overline{\mathbf{T}}_e^{G'}] \\ \mathbf{H}_e^{T2V} = \text{avg}(\sum_{k=1}^K (\text{Softmax}(\omega_k \otimes \mathbf{h}_e^{T2V}) \otimes \mathbf{h}_e^{T2V})) \\ \mathcal{M}_e^{T2V} = \mathbf{H}_e^{T2V} \oplus \text{Tanh}(\mathbf{T}_e^G) \otimes \mathbf{T}_e^G \end{cases} \quad (7)$$

where  $\text{Concat}[\circ; \circ]$  and  $\text{avg}(\circ)$  denote the concatenation and average operation, respectively.  $\text{Tanh}(\circ)$  is an activation function,  $K$  represents the number of heads,  $\oplus$  denotes the element-wise addition,  $\otimes$  is the algebraic multiplication operation, and  $\omega_k > 0$  is the temperature controlling the sharpness of scores. It should be noted that before executing the Concat operation, the dimensions of  $\overline{\mathbf{T}}_e^{G'}$  need to be expanded to convert it from  $\mathbf{T}_e^{G'} \in \mathbb{R}^{d_c}$  to  $\overline{\mathbf{T}}_e^{G'} \in \mathbb{R}^{1 \times d_c}$ .

- (3) Analogously, taking the mention global textual feature  $\mathbf{T}_m^G$  and mention local visual features  $\mathbf{V}_m^L$  as inputs, after going through Step 1 and Step 2 above, we obtain the mention-level textual-to-visual matching representation  $\mathcal{M}_m^{T2V}$ . The textual-to-visual matching score  $\mathcal{M}^{T2V}$  is then calculated as follows:

$$\mathcal{M}^{T2V} = \mathcal{M}_e^{T2V} \odot \mathcal{M}_m^{T2V} \quad (8)$$

In the same way, we can obtain the entity-level visual-to-textual matching representation  $\mathcal{M}_e^{V2T}$  and the mention-level visual-to-textual matching embedding  $\mathcal{M}_m^{V2T}$ . We can also apply the dot product of  $\mathcal{M}_e^{V2T}$  and  $\mathcal{M}_m^{V2T}$  to get the visual-to-textual matching score  $\mathcal{M}^{V2T}$ . Finally, we combine the textual-to-visual score and the visual-to-textual score to get the cross-modal matching network result  $\mathcal{M}_C = (\mathcal{M}_m^{T2V} + \mathcal{M}_m^{V2T})/2$ .

### 3.5 Joint Training

Consider the textual intra-modal matching score  $\mathcal{M}_T$  and the visual intra-modal matching score  $\mathcal{M}_V$  from the IMN module and the cross-modal matching score  $\mathcal{M}_C$  from the CMN module. We can obtain the union matching score as  $\mathcal{M}_U = (\mathcal{M}_T + \mathcal{M}_V + \mathcal{M}_C)/3$ . We select the Unit-Consistent Objective Function [28]  $\mathcal{L}_{uco}$  as the basic loss function. Specifically, the entire joint training process loss  $\mathcal{L}_{Joint}$  contains three aspects of loss contents as shown in Equation 9: *i*) the intra-modal contrastive learning loss  $\mathcal{L}_{cl}$ ; *ii*) the union matching loss  $\mathcal{L}_U = \mathcal{L}_{uco}(\mathcal{M}_U)$ ; *iii*) to avoid the whole model to excessively rely on the union score, we also introduce the independent intra-model textual loss  $\mathcal{L}_T = \mathcal{L}_{uco}(\mathcal{M}_T)$ , the intra-modal visual loss  $\mathcal{L}_V = \mathcal{L}_{uco}(\mathcal{M}_V)$ , and the cross-modal loss  $\mathcal{L}_C = \mathcal{L}_{uco}(\mathcal{M}_C)$ .

$$\mathcal{L}_{Joint} = \mathcal{L}_{cl} + \mathcal{L}_U + \mathcal{L}_T + \mathcal{L}_V + \mathcal{L}_C \quad (9)$$

## 4 EXPERIMENTS

To evaluate the effectiveness of M<sup>3</sup>EL, we conduct the following four experiments: including main results, ablation studies, parameter sensitivity (see [Appendix A](#)), and additional experiments (see [Appendix B](#)).

### 4.1 Experimental Setup

► **Datasets.** We evaluate the M<sup>3</sup>EL model on three well-known datasets: WikiMEL [40], RichpediaMEL [40], and WikiDiverse [41]. WikiMEL has more than 22K multimodal samples, where entities come from WikiData [38] and their corresponding textual and visual descriptions from Wikipedia. RichpediaMEL has more than 17K multimodal samples, where the entity ids are from the large-scale multimodal knowledge graph Richpedia [39] and the corresponding multimodal information from Wikipedia. WikiDiverse has more than 7k multimodal samples, constructed from WikiNews. For fair comparison, we adopt the dataset division ratio from MIMIC [28]. The statistics of these datasets are shown in Table 1.

**Table 1: Statistics of three different datasets. "Num." and "Img." denote number and image, respectively.**

Statistics	WikiMEL	RichpediaMEL	WikiDiverse
# Num. of sentences	22,070	17,724	7,405
# Num. of entities	109,976	160,935	132,460
# entities with Img.	67,195	86,769	67,309
# Num. of mentions	25,846	17,805	15,093
# Img. of mentions	22,136	15,853	6,697
# mentions in train	18,092	12,463	11,351
# mentions in valid	2,585	1,780	1,664
# mentions in test	5,169	3,562	2,078

► **Evaluation Metrics.** We evaluate the performance using two common metrics: MRR and Hits@N. MRR defines the inverse of the rank for the first correct answer, Hits@N is the proportion of correct answers ranked in the top N, with  $N=\{1,3,5\}$ . The higher the values of MRR or Hits@N, the better the performance.

► **Implementation Details.** We conduct all experiments on six 32G Tesla V100 GPUs, and use the AdamW [27] optimizer. Following MIMIC [28], we employ the pre-trained CLIP-Vit-Base-Patch32 model<sup>1</sup> as the initialization textual and visual encoder. For the textual modality, we set the maximal input length of the text to 40 and the dimension of the textual output features  $d_t$  to 512. For the visual modality, we rescale all the images into a 224×224 resolution and set the dimension of the visual output features  $d_o$  to 96. The scaled dimension size  $d_s$  is set to 96 and the patch size  $P$  is set to 32. We use grid search to select the optimal hyperparameters, mainly including: the learning rate  $lr \in \{5e-6, \mathbf{1e-5}, 2e-5, 3e-5, 4e-5\}$ , the batch size  $bs \in \{48, 64, 80, \mathbf{96}, 112\}$ , the temperature coefficient  $\tau \in \{\mathbf{0.03}, 0.10, 0.25, 0.5, 0.75\}$  in Equation 2, the number of heads  $K \in \{3, 4, 5, 6, 7\}$ , the inner-source alignment weight  $\beta \in \{0.2, 0.4, 0.6, \mathbf{0.8}, 1.0\}$ , the inter-source alignment weight  $\gamma \in \{0.2, 0.4, 0.6, 0.8, \mathbf{1.0}\}$ .

► **Baselines.** We compare M<sup>3</sup>EL with three types of baselines. *(i)* textual-based methods, including BLINK [42], BERT [8] and RoBERTa [25]; *(ii)* representation learning frameworks, including DZMNE [29], JMEL [1], VELML [50] and GHMFC [40]; *(iii)* vision-and-language-based methods, including CLIP [33], ViLT [19], ALBEF [23], METER [9] and MIMIC [28]; *(iv)* generative-based methods, including GPT-3.5-Turbo [30] and GEMEL [36].

<sup>1</sup><https://huggingface.co/openai/clip-vit-base-patch32>

**Table 2: Evaluation of different models on three MEL datasets, all the baselines results are from the MIMIC [28] paper. Best scores are highlighted in bold, the second best scores are underlined. It should be noted that there are a large number of - labeled results in GPT-3.5-Turbo and GEMEL. The main reasons are, on the one hand, [36] only provides results for the WikiMEL and WikiDiverse datasets, and the WikiDiverse dataset is completely different from that used by other baselines. [36] only uses Hits@1 as the evaluation indicator.**

Methods	WikiMEL				RichpediaMEL				WikiDiverse			
	MRR	Hits@1	Hits@3	Hits@5	MRR	Hits@1	Hits@3	Hits@5	MRR	Hits@1	Hits@3	Hits@5
BLINK [42]	81.72	74.66	86.63	90.57	71.39	58.47	81.51	88.09	69.15	57.14	78.04	85.32
BERT [8]	81.78	74.82	86.79	90.47	71.67	59.55	81.12	87.16	67.38	55.77	75.73	83.11
RoBERTa [25]	80.86	73.75	85.85	89.80	72.80	61.34	81.56	87.15	70.52	59.46	78.54	85.08
DZMNED [29]	84.97	78.82	90.02	92.62	76.63	68.16	82.94	87.33	67.59	56.90	75.34	81.41
JMEL [1]	73.39	64.65	79.99	84.34	60.06	48.82	66.77	73.99	48.19	37.38	54.23	61.00
VELML [50]	83.42	76.62	88.75	91.96	77.19	67.71	84.57	89.17	66.13	54.56	74.43	81.15
GHMFC [40]	83.36	76.55	88.40	92.01	80.76	72.92	86.85	90.60	70.99	60.27	79.40	84.74
CLIP [33]	88.23	83.23	92.10	94.51	77.57	67.78	85.22	90.04	71.69	61.21	79.63	85.18
ViLT [19]	79.46	72.64	84.51	87.86	56.63	45.85	62.96	69.80	45.22	34.39	51.07	57.83
ALBEF [23]	84.56	78.64	88.93	91.75	75.29	65.17	82.84	88.28	69.93	60.59	75.59	81.30
METER [9]	79.49	72.46	84.41	88.17	74.15	63.96	82.24	87.08	63.71	53.14	70.93	77.59
MIMIC [28]	<u>91.82</u>	87.98	95.07	96.37	86.95	81.02	91.77	94.38	73.44	63.51	81.04	86.43
GPT-3.5-Turbo [30]	-	73.80	-	-	-	-	-	-	-	-	-	-
GEMEL [36]	-	82.60	-	-	-	-	-	-	-	-	-	-
M <sup>3</sup> EL <sub>attr</sub>	<b>92.30</b>	<u>88.49</u>	<b>95.55</b>	<b>97.10</b>	<u>88.08</u>	<u>82.79</u>	<u>92.53</u>	<u>94.69</u>	<u>77.26</u>	<u>68.77</u>	<u>83.59</u>	<u>87.58</u>
M <sup>3</sup> EL <sub>desc</sub>	<b>92.30</b>	<b>88.84</b>	<u>95.20</u>	<u>96.71</u>	<b>88.26</b>	<b>82.82</b>	<b>92.73</b>	<b>95.34</b>	<b>81.29</b>	<b>74.06</b>	<b>86.57</b>	<b>90.04</b>

**Table 3: Evaluation of different models in low resource settings on four datasets. All the baselines results are from the MIMIC [28] paper. Best scores are highlighted in bold, the second best scores are underlined. H@i is the abbreviation of Hits@i.**

Methods	RichpediaMEL(10%)				RichpediaMEL(20%)				WikiDiverse(10%)				WikiDiverse(20%)			
	MRR	H@1	H@3	H@5	MRR	H@1	H@3	H@5	MRR	H@1	H@3	H@5	MRR	H@1	H@3	H@5
DZMNED [29]	31.79	22.57	34.95	41.33	47.01	36.38	52.25	58.28	19.99	11.45	22.52	29.50	40.97	28.73	47.35	56.69
JMEL [1]	25.01	16.70	27.68	33.63	39.38	28.92	43.35	50.59	28.26	19.97	32.19	37.58	39.05	29.26	44.23	49.90
VELML [50]	35.52	27.15	38.60	43.99	59.24	48.85	64.91	71.76	40.70	30.51	46.20	52.36	54.76	43.65	61.36	67.66
GHMFC [40]	76.69	<u>68.00</u>	83.38	87.73	80.42	72.57	86.69	90.15	59.56	48.08	66.31	74.25	63.46	51.73	71.85	78.54
CLIP [33]	72.51	62.66	79.14	85.06	73.72	64.32	79.59	85.54	69.49	59.87	76.52	81.57	69.95	59.96	77.05	82.24
ViLT [19]	17.05	11.73	18.59	22.07	38.81	30.24	42.39	48.40	19.57	13.19	21.27	26.37	29.48	20.93	32.92	38.93
ALBEF [23]	72.51	63.19	79.31	84.25	73.02	64.21	79.47	85.32	62.26	51.83	69.20	74.64	66.56	56.40	73.87	78.97
METER [9]	71.40	60.89	79.23	84.78	71.82	61.51	79.56	84.48	53.53	40.42	61.31	70.26	53.46	40.23	61.16	70.45
MIMIC [28]	74.62	64.49	82.03	87.59	<b>82.73</b>	<b>75.60</b>	<b>88.63</b>	<u>91.72</u>	69.70	60.54	76.18	81.33	63.46	61.01	77.67	83.35
M <sup>3</sup> EL <sub>attr</sub>	<u>77.24</u>	67.41	<u>84.87</u>	<u>89.25</u>	81.53	73.33	88.01	91.61	<u>73.80</u>	<u>65.88</u>	<u>78.83</u>	<u>83.73</u>	<u>75.23</u>	<u>67.08</u>	<u>80.56</u>	<u>85.32</u>
M <sup>3</sup> EL <sub>desc</sub>	<b>78.68</b>	<b>69.54</b>	<b>85.77</b>	<b>89.70</b>	<u>82.04</u>	<u>74.20</u>	<u>88.32</u>	<b>91.89</b>	<b>74.61</b>	<b>66.36</b>	<b>80.70</b>	<b>84.31</b>	<b>77.90</b>	<b>70.36</b>	<b>83.16</b>	<b>87.63</b>

## 4.2 Main Results

We conduct experiments on the WikiMEL, RichpediaMEL and WikiDiverse datasets in the normal and low resource settings. The corresponding results are shown in Tables 2 and 3.

► **Overall Performance Comparison.** Table 2 presents results of the performance of M<sup>3</sup>EL and the baselines on the WikiMEL, RichpediaMEL and WikiDiverse datasets. We consider two variants

of M<sup>3</sup>EL, M<sup>3</sup>EL<sub>attr</sub> and M<sup>3</sup>EL<sub>desc</sub>, which differ in the available textual knowledge. For M<sup>3</sup>EL<sub>attr</sub>, following MIMIC, we use the entity attribute knowledge as the textual content of the corresponding entity. For M<sup>3</sup>EL<sub>desc</sub>, we use the textual description of the entity in WikiData<sup>2</sup> as its textual modal content. The main motivation for replacing attribute knowledge with the description knowledge from Wikidata is that the word length of the description is larger than

<sup>2</sup><https://query.wikidata.org/>

that of the textual attribute, providing richer textual modal content. Under the same experimental conditions, we observe that  $M^3EL_{attr}$  outperforms existing SoTA baselines by a large margin across all metrics. We have three main findings: (1) Compared with the best performing baseline, MIMIC,  $M^3EL_{attr}$  respectively achieves 0.48% and 0.51% improvements in MRR and Hits@1 on the WikiMEL dataset. A similar behavior is observed on the RichpediaMEL and WikiDiverse datasets. (2) On the three datasets, when compared with MIMIC, the improvement on the Hits@1 metric is higher than that on the Hits@3 metric, which shows that our  $M^3EL_{attr}$  pays more attention to highly accurate matching in the multimodal entity linking task. (3) The use of description knowledge further improves the performance: on the three datasets, the performance of  $M^3EL_{desc}$  is better than that of  $M^3EL_{attr}$ . The bigger gain is in the WikiDiverse dataset. The main reason is that in the WikiDiverse dataset, a large percentage of the entities have short text descriptions, with the average text word length being only 1.24. After replacing attribute knowledge with description knowledge, the average word length of the entity text corresponding to the mention becomes 4.50. Therefore, we believe that the availability of textual knowledge is one of the important factors affecting the model performance. If there is no special explanation,  $M^3EL$  appearing in subsequent parts will uniformly refer to  $M^3EL_{desc}$ .

► **Low Resource Setting.** To better understand the performance of  $M^3EL$  and existing baselines in low-resource scenarios, we conducted experiments on the RichpediaMEL and WikiDiverse datasets with 10% and 20% of the training data, while keeping the validation and test sets unchanged. The corresponding results are presented in Table 3. We observe that  $M^3EL$  consistently achieves optimal performance on almost all subsets. We have the following two main findings. 1) Except for the case when only 20% of the RichpediaMEL training data is used,  $M^3EL$  achieves optimal performance. Note that there is no unique best performing (second overall) baseline, switching between GHMFC, CLIP and MIMIC. This phenomenon reveals that  $M^3EL$  is more stable and can adapt to a variety of datasets under different conditions. In fact, in the RichpediaMEL (20%) scenario,  $M^3EL$  also achieves competitive results. 2) On the WikiDiverse dataset as the training proportion increases, the gap between  $M^3EL$  and MIMIC gradually becomes larger. We attribute this performance improvement to the fact that the intra-modal contrastive learning module is able to obtain better discriminative representations as the size of the training data increases. The additional support of the multi-level matching mechanism of intra-modal and inter-modal has further brought a positive impact of final results.

### 4.3 Ablation Studies

We conduct ablation experiments on the WikiMEL, RichpediaMEL and WikiDiverse datasets under different conditions. Table 4 presents results showing the contribution of each component of  $M^3EL$ . These include the following three points: *a*) removing one of  $\mathcal{L}_U$ ,  $\mathcal{L}_T$ ,  $\mathcal{L}_V$ ,  $\mathcal{L}_C$  or  $\mathcal{L}_{cl}$  from the loss function  $\mathcal{L}_{Joint}$ ; *b*) removing the textual intra-modal matching module (w/o  $\mathcal{L}_T + \mathcal{M}_T$ ), the visual intra-modal matching module (w/o  $\mathcal{L}_V + \mathcal{M}_V$ ), or the cross-modal matching module (w/o  $\mathcal{L}_C + \mathcal{M}_C$ ) from  $M^3EL$ , it should be noted

that there is no ablation scenario w/o  $\mathcal{M}_T$ , w/o  $\mathcal{M}_V$ , w/o  $\mathcal{M}_C$ , because  $\mathcal{L}_T$ ,  $\mathcal{L}_V$ ,  $\mathcal{L}_C$  are calculated based on  $\mathcal{M}_T$ ,  $\mathcal{M}_V$ ,  $\mathcal{M}_C$ , and removing  $\mathcal{M}_T$ ,  $\mathcal{L}_V$ ,  $\mathcal{L}_C$  would mean that  $\mathcal{L}_T$ ,  $\mathcal{L}_V$ ,  $\mathcal{L}_C$  are also removed; *c*) replacing ICL with two contrastive learning losses, i.e., w/ InfoNCE [14] and w/ MCLET [16]. In addition, we also conduct experiments Effect of Different Pooling Operation in Equation 5 and Resource Consumption Using Various Contrastive Loss.

► **Impact of Different Losses.** The upper part of Table 4 shows the individual contribution of different losses. We can observe that remove any loss will generally bring certain degree of performance degradation. On the RichpediaMEL and WikiDiverse datasets, the performance loss caused by removing the visual loss is higher than by removing the textual loss. However, on the WikiMEL dataset, the situation is the opposite, i.e., the performance fluctuation caused by removing the textual loss is larger. This shows that the richness of modal knowledge is the main factor that determines the impact of the corresponding modality on model performance. In addition, removing the contrastive loss also has certain impact on performance, especially on the WikiDiverse dataset. This is mainly due to the fact that we also consider the negative examples within a modality in the contrastive learning process to obtain better discriminative modal embedding representations. Although there are some singularities in some indicators of some datasets when  $\mathcal{L}_T$ ,  $\mathcal{L}_V$ ,  $\mathcal{L}_C$  are removed, this is acceptable because the information richness of textual and visual modalities in each dataset is different. Indiscriminately removing modules for specific modalities will cause unknown performance losses. The overall performance is the best when all losses and modules are simultaneously used.

► **Impact of Different Modules.** The middle part of Table 4 shows the individual contribution of different modules. It should be mentioned that removing the corresponding module involves removing two aspects: for example, when removing the cross-modal matching network (CMN), the matching score  $\mathcal{M}_C$  related to the CMN module needs to be removed from the union matching score  $\mathcal{M}_U$ , and the loss  $\mathcal{L}_C$  introduced by  $\mathcal{M}_C$  also needs to be removed. Since the loss is calculated from the matching score of the corresponding module, there will be no corresponding loss value without a matching score. From the experimental results in Table 4, we can observe that when compared to only removing the loss value  $\mathcal{L}_C$  related to the corresponding module, removing the matching score of the that module from the union matching score will lead to a greater performance degradation. Taking the textual modality of the WikiMEL dataset as an example, if only the textual modality loss is removed, the corresponding MRR and Hits@1 metrics respectively are 91.64 and 87.60. After further removing the matching score  $\mathcal{M}_T$  related to the textual modality, the corresponding MRR and Hits@1 metrics become 90.22 and 86.40, falling by 1.42% and 1.2% respectively. A similar situation occurs when modules related to visual modalities and cross-modalities are removed, which confirms the usefulness of each module.

► **Impact of Various Contrastive Loss.** The lower part of Table 4 shows the experimental results of replacing the ICL module with the InfoNCE [14] and MCLET [16] contrastive losses. We can observe that with our ICL’s  $M^3EL$  can achieve better experimental results in most cases. Specifically, taking the WikiMEL dataset as an example, compared with InfoNCE and MCLET, the ICL module improves the



**Table 4: Evaluation of ablation studies on three MEL datasets. Best scores are highlighted in bold, the second best scores are underlined.**

Methods	WikiMEL				RichpediaMEL				WikiDiverse			
	MRR	Hits@1	Hits@3	Hits@5	MRR	Hits@1	Hits@3	Hits@5	MRR	Hits@1	Hits@3	Hits@5
w/o $\mathcal{L}_U$	91.62	87.81	94.53	96.40	<b>88.34</b>	<u>83.27</u>	92.59	94.50	75.46	66.12	82.44	87.15
w/o $\mathcal{L}_T$	91.64	87.60	94.97	96.67	85.62	78.66	91.58	94.41	80.63	<u>73.68</u>	86.00	88.74
w/o $\mathcal{L}_V$	<u>92.06</u>	<u>88.37</u>	<b>95.20</b>	96.54	85.27	78.94	90.40	93.12	78.00	69.83	83.83	88.50
w/o $\mathcal{L}_C$	90.91	86.79	94.22	96.19	86.55	80.32	91.72	94.53	<u>80.76</u>	73.34	<b>86.86</b>	<u>89.85</u>
w/o $\mathcal{L}_{cl}$	91.89	88.35	94.74	96.42	88.23	<b>83.63</b>	91.66	94.08	75.66	66.31	82.68	87.82
w/o $\mathcal{L}_T+\mathcal{M}_T$	90.22	86.40	93.05	95.03	84.71	78.38	89.64	92.56	67.46	59.43	73.10	77.19
w/o $\mathcal{L}_V+\mathcal{M}_V$	87.37	81.72	91.78	94.27	81.85	73.64	88.69	92.25	78.32	69.63	85.90	89.46
w/o $\mathcal{L}_C+\mathcal{M}_C$	91.63	87.54	<u>95.12</u>	96.70	87.00	81.08	91.89	94.33	78.32	69.63	85.90	89.46
w/ InfoNCE [14]	90.54	86.28	94.06	96.03	85.29	79.06	90.26	93.07	79.87	72.62	85.61	88.74
w/ MCLET [16]	91.85	87.79	<b>95.20</b>	<b>96.77</b>	87.69	81.78	<u>92.67</u>	<u>95.03</u>	79.95	72.18	86.00	89.61
M <sup>3</sup> EL	<b>92.30</b>	<b>88.84</b>	<b>95.20</b>	<u>96.71</u>	<u>88.26</u>	82.82	<b>92.73</b>	<b>95.34</b>	<b>81.29</b>	<b>74.06</b>	<u>86.57</u>	<b>90.04</b>

MRR metric by 1.84% and 0.45%, respectively. This is due to the fact that we consider both inner-source and inter-source negative samples in the ICL module. In addition, we introduce a weight coefficient in Equation 2 to reconcile the possible imbalance of negative samples. We conduct parameter analysis experiments on the effect of inner-source and inter-source alignment weights  $\beta$  and  $\gamma$  in [Appendix A](#).

**Table 5: Evaluation of ablation studies of different pooling operation on WikiDiverse dataset.**

Methods	WikiDiverse			
	MRR	Hits@1	Hits@3	Hits@5
<i>max</i>	77.28	68.86	83.73	87.63
<i>soft</i>	77.39	69.01	83.78	87.82
<i>mean</i>	<b>81.29</b>	<b>74.06</b>	<b>86.57</b>	<b>90.04</b>

► **Effect of Different Pooling Operation in Equation 5.** The mean pooling operation in Equation 5 is mainly used to reduce the spatial dimension of  $\alpha^L$  to facilitate its calculation with  $\mathbf{T}_e^G$  to obtain the global-to-local matching score  $\mathcal{M}_T^{G2L}$ . We replace the mean pooling operation with max pooling and soft pooling [31] operations on the WikiDiverse dataset to study the impact of the pooling operation. The corresponding results are shown in Table 5. We find that the advantage of using mean pooling operation is more prominent. A possible explanation is that it is more effective to comprehensively consider the representation of each token in a sentence or each patch in an image than to consider only some important tokens or patches.

► **Resource Consumption Using Various Contrastive Loss.** We analyze the resource consumption from two perspectives: time complexity and space complexity. The corresponding results on three different datasets are shown in the Table 6. The time complexity is measured by the number of floating-point operations (#FLOPs) required during training phase, while the space complexity refers to the amount of a models parameters (#Params). The larger the

**Table 6: Amount of parameters and calculation with various contrastive loss.**

Metrics	Mode	WikiMEL	RichpediaMEL	WikiDiverse
#FLOPs	InfoNCE	1.469G	1.469G	2.233G
	MCLET	1.402G	1.402G	2.128G
	ICL	<b>1.369G</b>	<b>1.369G</b>	<b>2.076G</b>
#Params	InfoNCE	335.259K	335.259K	324.753K
	MCLET	321.423K	321.423K	311.721K
	ICL	<b>314.529K</b>	<b>314.529K</b>	<b>305.217K</b>

values of #FLOPs and #Params are, the more computing power and higher memory usage are required during the training process. We observe that compared with InfoNCE and MCLET, ICL requires less time and space overhead in each dataset. Specifically, on the WikiMEL dataset, ICL reduces #FLOPs and #Params by 2.4% and 2.1%, respectively, compared to MCLET, which demonstrates that ICL is more efficient.

## 5 CONCLUSION

In this paper, we propose M<sup>3</sup>EL, a multi-level matching network for multimodal entity linking. M<sup>3</sup>EL simultaneously considers the diversity of negative samples from the same modality and bidirectional cross-modality interaction. Specifically, we introduce an intra-modal contrastive loss to obtain better discriminative representations that are faithful to certain modality. Furthermore, we design intra-modal and inter-modal matching mechanisms to explore multi-level multimodal interactions. Extensive experiments on three datasets demonstrate M<sup>3</sup>EL’s robust performance.

## ACKNOWLEDGMENTS

This work has been supported by the National Natural Science Foundation of China (No.61936012, No.62076155), by the Key Research and Development Project of Shanxi Province (No.202102020101008), by the Science and Technology Cooperation and Exchange Special Project of Shanxi Province (No.202204041101016).

## REFERENCES

- [1] Omar Adjali, Romaric Besançon, Olivier Ferret, Hervé Le Borgne, and Brigitte Grau. 2020. Multimodal Entity Linking for Tweets. In *ECIR*. Springer, Lisbon, Portugal, 463–478.
- [2] Ali Ahmadvand, Harshita Sahijwani, Jason Ingyu Choi, and Eugene Agichtein. 2019. ConCET: Entity-Aware Topic Classification for Open-Domain Conversational Agents. In *CIKM*. ACM, Beijing, China, 1371–1380.
- [3] Alex Andonian, Shixing Chen, and Raffay Hamid. 2022. Robust Cross-Modal Representation Learning with Progressive Self-Distillation. In *CVPR*. IEEE, New Orleans, LA, USA, 16409–16420.
- [4] Ilaria Bordino, Yelena Mejova, and Mounia Lalmas. 2013. Penguins in sweaters, or serendipitous entity search on user-generated content. In *CIKM*. ACM, San Francisco, CA, USA, 109–118.
- [5] Nicola De Cao, Gautier Izacard, Sebastian Riedel, and Fabio Petroni. 2021. Autoregressive Entity Retrieval. In *ICLR*. OpenReview.net, online, 1–20.
- [6] Yixin Cao, Lei Hou, Juanzi Li, and Zhiyuan Liu. 2018. Neural Collective Entity Linking. In *COLING*. ACL, Santa Fe, New Mexico, USA, 675–686.
- [7] Tao Cheng, Xifeng Yan, and Kevin Chen-Chuan Chang. 2007. EntityRank: Searching Entities Directly and Holistically. In *VLDB*. ACM, Vienna, Austria, 387–398.
- [8] Jacob Devlin, Ming-Wei Chang, Kenton Lee, and Kristina Toutanova. 2019. BERT: Pre-training of Deep Bidirectional Transformers for Language Understanding. In *NAACL*. ACL, Minneapolis, MN, USA, 4171–4186.
- [9] Zi-Yi Dou, Yichong Xu, Zhe Gan, Jianfeng Wang, Shuohang Wang, Lijuan Wang, Chenguang Zhu, Pengchuan Zhang, Lu Yuan, Nanyun Peng, Zicheng Liu, and Michael Zeng. 2022. An Empirical Study of Training End-to-End Vision-and-Language Transformers. In *CVPR*. IEEE, New Orleans, LA, USA, 18145–18155.
- [10] Zheng Fang, Yanan Cao, Qian Li, Dongjie Zhang, Zhenyu Zhang, and Yanbing Liu. 2019. Joint Entity Linking with Deep Reinforcement Learning. In *WWW*. ACM, San Francisco, CA, USA, 438–447.
- [11] Octavian-Eugen Ganea and Thomas Hofmann. 2017. Deep Joint Entity Disambiguation with Local Neural Attention. In *EMNLP*. ACL, Copenhagen, Denmark, 2619–2629.
- [12] Xiaoqi Han, Ru Li, Xiaoli Li, Jiye Liang, Zifang Zhang, and Jeff Z. Pan. 2024. InstructEd: Soft-Instruction Tuning for Model Editing with Hops. In *ACL*. ACL, Bangkok, Thailand, 14953–14968.
- [13] Bowei He, Xu He, Yingxue Zhang, Ruiming Tang, and Chen Ma. 2023. Dynamically Expandable Graph Convolution for Streaming Recommendation. In *WWW*. ACM, Austin, TX, USA, 1457–1467.
- [14] Kaiming He, Haoqi Fan, Yuxin Wu, Saining Xie, and Ross B. Girshick. 2020. Momentum Contrast for Unsupervised Visual Representation Learning. In *CVPR*. IEEE, Seattle, WA, USA, 9726–9735.
- [15] Johannes Hoffart, Mohamed Amir Yosef, Ilaria Bordino, Hagen Fürstenau, Manfred Pinkal, Marc Spaniol, Bilyana Taneva, Stefan Thater, and Gerhard Weikum. 2011. Robust Disambiguation of Named Entities in Text. In *EMNLP*. ACL, Edinburgh, UK, 782–792.
- [16] Zhiwei Hu, Víctor Gutiérrez-Basulto, Zhiliang Xiang, Ru Li, and Jeff Z. Pan. 2023. Multi-view Contrastive Learning for Entity Typing over Knowledge Graphs. In *EMNLP*. ACL, Singapore, 12950–12963.
- [17] Zhiwei Hu, Víctor Gutiérrez-Basulto, Zhiliang Xiang, Ru Li, and Jeff Z. Pan. 2024. Leveraging Intra-modal and Inter-modal Interaction for Multi-Modal Entity Alignment. *CoRR* abs/2404.17590 (2024). arXiv:2404.17590
- [18] Zhiwei Hu, Víctor Gutiérrez-Basulto, Zhiliang Xiang, Xiaoli Li, Ru Li, and Jeff Z. Pan. 2022. Type-aware Embeddings for Multi-Hop Reasoning over Knowledge Graphs. In *IJCAI*. ijcai.org, Vienna, Austria, 3078–3084.
- [19] Wonjae Kim, Bokyoung Son, and Ildoo Kim. 2021. ViLT: Vision-and-Language Transformer Without Convolution or Region Supervision. In *ICML*. PMLR, online, 5583–5594.
- [20] Phong Le and Ivan Titov. 2018. Improving Entity Linking by Modeling Latent Relations between Mentions. In *ACL*. ACL, Melbourne, Australia, 1595–1604.
- [21] Junnan Li, Dongxu Li, Silvio Savarese, and Steven C. H. Hoi. 2023. BLIP-2: Bootstrapping Language-Image Pre-training with Frozen Image Encoders and Large Language Models. In *ICML*. PMLR, Honolulu, Hawaii, USA, 19730–19742.
- [22] Junnan Li, Dongxu Li, Caiming Xiong, and Steven C. H. Hoi. 2022. BLIP: Bootstrapping Language-Image Pre-training for Unified Vision-Language Understanding and Generation. In *ICML*. PMLR, Baltimore, Maryland, USA, 12888–12900.
- [23] Junnan Li, Ramprasaath R. Selvaraju, Akhilesh Gotmare, Shafiq R. Joty, Caiming Xiong, and Steven Chu-Hong Hoi. 2021. Align before Fuse: Vision and Language Representation Learning with Momentum Distillation. In *NeurIPS*. Curran Associates, online, 9694–9705.
- [24] Lizi Liao, Yunshan Ma, Xiangnan He, Richang Hong, and Tat-Seng Chua. 2018. Knowledge-aware Multimodal Dialogue Systems. In *MM*. ACM, Seoul, Republic of Korea, 801–809.
- [25] Yinhan Liu, Myle Ott, Naman Goyal, Jingfei Du, Mandar Joshi, Danqi Chen, Omer Levy, Mike Lewis, Luke Zettlemoyer, and Veselin Stoyanov. 2019. RoBERTa: A Robustly Optimized BERT Pretraining Approach. *CoRR* abs/1907.11692 (2019), 1–13.
- [26] Shayne Longpre, Kartik Perisetla, Anthony Chen, Nikhil Ramesh, Chris DuBois, and Sameer Singh. 2021. Entity-Based Knowledge Conflicts in Question Answering. In *EMNLP*. ACL, online, 7052–7063.
- [27] Ilya Loshchilov and Frank Hutter. 2019. Decoupled Weight Decay Regularization. In *ICLR*. OpenReview.net, New Orleans, LA, USA, 1–11.
- [28] Pengfei Luo, Tong Xu, Shiwei Wu, Chen Zhu, Linli Xu, and Enhong Chen. 2023. Multi-Grained Multimodal Interaction Network for Entity Linking. In *KDD*. ACM, Long Beach, CA, USA, 1583–1594.
- [29] Seungwhan Moon, Leonardo Neves, and Vitor Carvalho. 2018. Multimodal Named Entity Disambiguation for Noisy Social Media Posts. In *ACL*. ACL, Melbourne, Australia, 2000–2008.
- [30] OpenAI. 2023. ChatGPT. <https://chat.openai.com>, 2023.
- [31] Weiran Pan, Wei Wei, and Xian-Ling Mao. 2021. Context-aware Entity Typing in Knowledge Graphs. In *EMNLP*. ACL, online, 2240–2250.
- [32] Matthew E. Peters, Mark Neumann, Robert L. Logan IV, Roy Schwartz, Vidur Joshi, Sameer Singh, and Noah A. Smith. 2019. Knowledge Enhanced Contextual Word Representations. In *EMNLP*. ACL, Hong Kong, China, 43–54.
- [33] Alec Radford, Jong Wook Kim, Chris Hallacy, Aditya Ramesh, Gabriel Goh, Sandhini Agarwal, Girish Sastry, Amanda Askell, Pamela Mishkin, Jack Clark, Gretchen Krueger, and Ilya Sutskever. 2021. Learning Transferable Visual Models From Natural Language Supervision. In *ICML*. PMLR, online, 8748–8763.
- [34] Chenwei Ran, Wei Shen, and Jianyong Wang. 2018. An Attention Factor Graph Model for Tweet Entity Linking. In *WWW*. ACM, Lyon, France, 1135–1144.
- [35] Wei Shen, Jianyong Wang, and Jiawei Han. 2015. Entity Linking with a Knowledge Base: Issues, Techniques, and Solutions. *TKDE* 27, 2 (2015), 443–460.
- [36] Senbao Shi, Zhenran Xu, Baotian Hu, and Min Zhang. 2024. Generative Multimodal Entity Linking. In *COLING*. ELRA and ICCL, Torino, Italy, 7654–7665.
- [37] Hugo Touvron, Louis Martin, Kevin Stone, Peter Albert, Amjad Almahairi, Yasmine Babaei, Nikolay Bashlykov, Soumya Batra, Prajwal Bhargava, Shruti Bhosale, Dan Bikel, Lukas Blecher, Cristian Canton-Ferrer, Moya Chen, Guillem Cucurull, David Esiobu, Jude Fernandes, Jeremy Fu, Wenyin Fu, Brian Fuller, Cynthia Gao, Vedanuj Goswami, Naman Goyal, Anthony Hartshorn, Saghar Hosseini, Rui Hou, Hakan Inan, Marcin Kardas, Viktor Kerkez, Madian Khabsa, Isabel Kloumann, Artem Korenev, Punit Singh Koura, Marie-Anne Lachaux, Thibaut Lavril, Jenya Lee, Diana Liskovich, Yinghai Lu, Yuning Mao, Xavier Martinet, Todor Mihaylov, Pushkar Mishra, Igor Molybog, Yixin Nie, Andrew Poulton, Jeremy Reizenstein, Rashi Rungta, Kalyan Saladi, Alan Schelten, Ruan Silva, Eric Michael Smith, Ranjan Subramanian, Xiaoqing Ellen Tan, Binh Tang, Ross Taylor, Adina Williams, Jian Xiang Kuan, Puxin Xu, Zheng Yan, Iliyan Zarov, Yuchen Zhang, Angela Fan, Melanie Kambadur, Sharan Narang, Aurélien Rodriguez, Robert Stojnic, Sergey Edunov, and Thomas Scialom. 2023. Llama 2: Open Foundation and Fine-Tuned Chat Models. *CoRR* abs/2307.09288 (2023). arXiv:2307.09288
- [38] Denny Vrandečić and Markus Krötzsch. 2014. Wikidata: a free collaborative knowledgebase. *Commun. ACM* 57, 10 (2014), 78–85.
- [39] Meng Wang, Haofen Wang, Guilin Qi, and Qiushuo Zheng. 2020. Richpedia: A Large-Scale, Comprehensive Multi-Modal Knowledge Graph. *Big Data Res.* 22 (2020), 100159.
- [40] Peng Wang, Jiangheng Wu, and Xiaohang Chen. 2022. Multimodal Entity Linking with Gated Hierarchical Fusion and Contrastive Training. In *SIGIR*. ACM, Madrid, Spain, 938–948.
- [41] Xuwu Wang, Junfeng Tian, Min Gui, Zhixu Li, Rui Wang, Ming Yan, Lihan Chen, and Yanghua Xiao. 2022. WikiDiverse: A Multimodal Entity Linking Dataset with Diversified Contextual Topics and Entity Types. In *ACL*. ACL, Dublin, Ireland, 4785–4797.
- [42] Ledell Wu, Fabio Petroni, Martin Josifoski, Sebastian Riedel, and Luke Zettlemoyer. 2020. Scalable Zero-shot Entity Linking with Dense Entity Retrieval. In *EMNLP*. ACL, online, 6397–6407.
- [43] Shangyu Xing, Fei Zhao, Zhen Wu, Chunhui Li, Jianbing Zhang, and Xinyu Dai. 2023. DRIN: Dynamic Relation Interactive Network for Multimodal Entity Linking. In *MM*. ACM, Ottawa, ON, Canada, 3599–3608.
- [44] Wenhan Xiong, Mo Yu, Shiyu Chang, Xiaoxiao Guo, and William Yang Wang. 2019. Improving Question Answering over Incomplete KBs with Knowledge-Aware Reader. In *ACL*. ACL, Florence, Italy, 4258–4264.
- [45] Zhichao Yan, Jiapu Wang, Jiaoyan Chen, Xiaoli Li, Ru Li, and Jeff Z. Pan. 2024. Atomic Fact Decomposition Helps Attributed Question Answering. *CoRR* abs/2410.16708 (2024), 1–17.
- [46] Chengmei Yang, Bowei He, Yimeng Wu, Chao Xing, Lianghua He, and Chen Ma. 2023. MMEL: A Joint Learning Framework for Multi-Mention Entity Linking. In *UAI*. PMLR, Pittsburgh, PA, USA, 2411–2421.
- [47] Jinyu Yang, Jiali Duan, Son Tran, Yi Xu, Sampath Chanda, Liqun Chen, Belinda Zeng, Trishul Chilimbi, and Junzhou Huang. 2022. Vision-Language Pre-Training with Triple Contrastive Learning. In *CVPR*. IEEE, New Orleans, LA, USA, 15650–15659.
- [48] Xiyuan Yang, Xiaotao Gu, Sheng Lin, Siliang Tang, Yuetting Zhuang, Fei Wu, Zhigang Chen, Guoping Hu, and Xiang Ren. 2019. Learning Dynamic Context Augmentation for Global Entity Linking. In *EMNLP*. ACL, Hong Kong, China, 271–281.

- [49] Wen-tau Yih, Ming-Wei Chang, Xiaodong He, and Jianfeng Gao. 2015. Semantic Parsing via Staged Query Graph Generation: Question Answering with Knowledge Base. In *ACL*. ACL, Beijing, China, 1321–1331.
- [50] Qishuo Zheng, Hao Wen, Meng Wang, and Guilin Qi. 2022. Visual Entity Linking via Multi-modal Learning. *Data Intell.* 4, 1 (2022), 1–19.
- [51] Yanqiao Zhu, Yichen Xu, Feng Yu, Qiang Liu, Shu Wu, and Liang Wang. 2021. Graph Contrastive Learning with Adaptive Augmentation. In *WWW*. ACM, online, 2069–2080.
- [52] Mohammadreza Zolfaghari, Yi Zhu, Peter V. Gehler, and Thomas Brox. 2021. CrossCLR: Cross-modal Contrastive Learning For Multi-modal Video Representations. In *ICCV*. IEEE, Montreal, QC, Canada, 1430–1439.

## APPENDIX

### A Parameter Sensitivity

We carry out parameter sensitivity experiments on the WikiMEL, RichpediaMEL and WikiDiverse datasets. The results are shown in Figure 4, including: *a)* effect of numbers of heads  $K$ ; *b)* effect of temperature coefficient  $\tau$ ; *c)* effect of inner-source and inter-source alignment weight  $\beta$  and  $\gamma$ .

► **Effect of Numbers of Heads  $K$ .** In Equation (7), we use a multi-head attention mechanism to achieve the fusion between cross-modal local features and the global feature. In Figure 4(a), we observe that the number of multi-head attention heads has a greater impact on the WikiMEL and RichpediaMEL datasets than on WikiDiverse. We achieve the best performance on all three datasets when the number is set to 5.

► **Effect of Temperature Coefficient  $\tau$ .** The temperature coefficient can be used to adjust the similarity measure between samples. When the temperature coefficient is higher, the model is more likely to reduce the difference between positive samples and negative samples. This can cause the learned feature representation to be less sensitive to the differences between different samples. When the temperature is lower, the model pays more attention to subtle differences between samples. This may lead to being overly sensitive to noise and local changes, thereby reducing the model’s generalization ability. Therefore, selecting an appropriate temperature coefficient value requires appropriate adjustments based on the characteristics of a dataset. We can see in Figure 4(b) that selecting a smaller temperature value is beneficial to all three datasets and the best results are achieved when the temperature value is set to 0.03.

► **Effect of Inner-source and Inter-source Alignment Weights  $\beta$  and  $\gamma$ .** The weight coefficients  $\beta$  and  $\gamma$  in Equation (2) can be used to control the importance of negative samples from inner-source and inter-source. An appropriate adjustment of the weights values, based on the dataset, can help avoiding the performance impact caused by improper selection of negative samples. We can observe in Figure 4(c) and (d) that selecting a larger  $\gamma$  value is more beneficial to the three datasets. However, there is no rule to follow for the selection of the  $\beta$  value because as  $\beta$  increases, the performance of the three datasets fluctuates.

### B Additional Experiments

► **Effect of Bidirectional Interaction Mechanism.** We conduct further ablation experiments on the T2V and V2T matching mechanisms of the CMN module in Section 3.4 on three datasets. The corresponding results are shown in Table 7. We can observe that using only the T2V or V2T matching mechanism will bring a certain

degree of performance degradation on the three datasets. Specifically, the performance loss caused by using only T2V is greater than that of using only V2T. Furthermore, on the WikiDiverse dataset, the performance degradation is the largest after removing T2V or V2T, which fully demonstrates the necessity of the two mechanisms. We further give the rational behind the existence of the two mechanisms. First, we need to give some explanations of terms. As described in Section 3.2.1, global textual feature refer to the embedding representation of the entire textual modality sentence, local textual features refers to the embedding representation of each token in the textual modality sentence, global visual feature refers to the embedding representation of the entire visual modality image, and local visual features refer to the embedding representation of each patch in the visual modality image. Secondly, for T2V, its input is global-textual feature and local visual features, *i.e.*, using the global representation at the sentence level to supervise the local representation at the image patch level, which is suitable for scenes with richer textual semantic knowledge, while V2T’s input is global visual feature and local textual features, which is more suitable for scenes with more visual information from the image. The T2V and V2T mechanisms are applicable to different scenarios. The combination of the two can complement each other and be more robust to changes in scenarios.

► **Effect of Different Feature Extractor.** We use CLIP as the feature extractor in MFE, mainly considering the following two factors: On the one hand, CLIP has good performance. On the other hand, the memory size of our experimental machine is limited, making it difficult to run larger models. In principle, CLIP can be replaced by any encoder that can obtain textual and visual modality embeddings, such as BLIP [22] or BLIP-2 [21]. Considering the current status of our experimental machine, we choose BLIP-vqa-base to replace CLIP for the experiment. The corresponding results are shown in Table 8. We find that using BLIP actually obtains worse results, the main reason is that in order to run the experiment, we performed float16 quantization on BLIP-vqa-base (otherwise the memory will overflow), which will lead to a large degree of precision loss. We leave experiments with full-scale runs of BLIP and BLIP-2 as future work.

► **Effect of Independent Mechanism in IMN Module.** To verify the performance of the independent mechanism proposed by the MIMIC [28] model on our M<sup>3</sup>EL model, we conduct experiments on the WikiMEL, RichpediaMEL, and WikiDiverse datasets. The corresponding results are shown in Table 9. We observe that after replacing our unified mechanism with an independent mechanism, there is a certain degree of performance loss on the three datasets, which illustrates that the independent mechanism is not suitable for M<sup>3</sup>EL. A possible explanation is that the interaction mechanism within the modality is similar, and there is no need to customize a unique interaction system for each modality. Instead, a simpler approach is more appropriate.

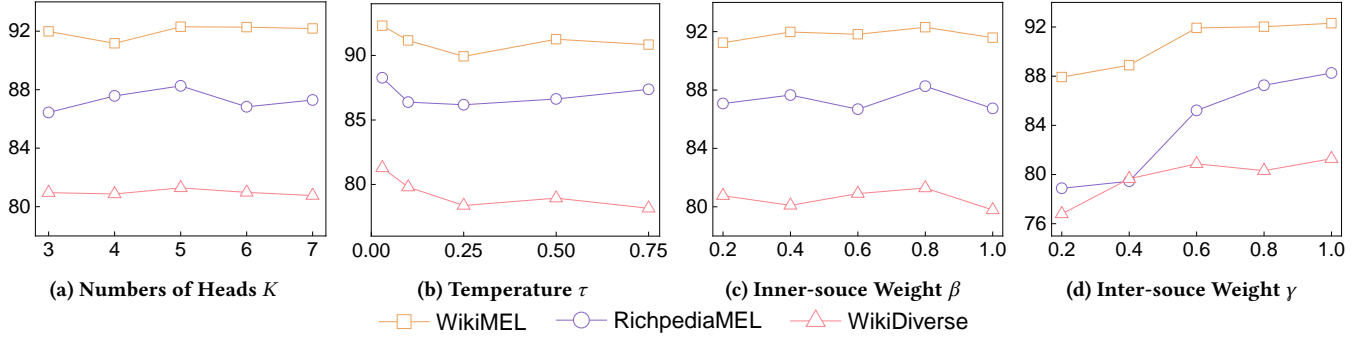


Figure 4: Parameter sensitivity experiments under different conditions on WikiMEL, RichpediaMEL and WikiDiverse datasets.

Table 7: Evaluation of ablation studies of T2V and V2T mechanism on WikiMEL, RichpediaMEL and WikiDiverse datasets.

Methods	WikiMEL				RichpediaMEL				WikiDiverse			
	MRR	Hits@1	Hits@3	Hits@5	MRR	Hits@1	Hits@3	Hits@5	MRR	Hits@1	Hits@3	Hits@5
w/ T2V	91.53	88.08	94.16	95.65	86.53	81.11	90.82	93.40	76.08	68.05	82.00	86.14
w/ V2T	91.80	88.24	94.76	96.32	87.89	81.96	91.75	94.27	76.73	67.95	84.12	87.58
w/ T2V & V2T	<b>92.30</b>	<b>88.84</b>	<b>95.20</b>	<b>96.71</b>	<b>88.26</b>	<b>82.82</b>	<b>92.73</b>	<b>95.34</b>	<b>81.29</b>	<b>74.06</b>	<b>86.57</b>	<b>90.04</b>

Table 8: Evaluation of ablation studies of different feature extractor on WikiMEL, RichpediaMEL and WikiDiverse datasets.

Methods	WikiMEL				RichpediaMEL				WikiDiverse			
	MRR	Hits@1	Hits@3	Hits@5	MRR	Hits@1	Hits@3	Hits@5	MRR	Hits@1	Hits@3	Hits@5
<i>BLIP</i>	58.05	51.13	62.00	65.76	41.55	33.13	45.90	50.95	36.85	27.19	41.92	49.23
<i>CLIP</i>	<b>92.30</b>	<b>88.84</b>	<b>95.20</b>	<b>96.71</b>	<b>88.26</b>	<b>82.82</b>	<b>92.73</b>	<b>95.34</b>	<b>81.29</b>	<b>74.06</b>	<b>86.57</b>	<b>90.04</b>

Table 9: Evaluation of ablation studies of independent mechanism in IMN module on WikiMEL, RichpediaMEL and WikiDiverse datasets.

Methods	WikiMEL				RichpediaMEL				WikiDiverse			
	MRR	Hits@1	Hits@3	Hits@5	MRR	Hits@1	Hits@3	Hits@5	MRR	Hits@1	Hits@3	Hits@5
<i>independent</i>	91.90	88.33	94.64	96.34	87.53	82.34	91.61	94.08	79.13	71.27	85.23	89.12
<i>same</i>	<b>92.30</b>	<b>88.84</b>	<b>95.20</b>	<b>96.71</b>	<b>88.26</b>	<b>82.82</b>	<b>92.73</b>	<b>95.34</b>	<b>81.29</b>	<b>74.06</b>	<b>86.57</b>	<b>90.04</b>